The 17th World Conference on Earthquake Engineering

17th World Conference on Earthquake Engineering, 17WCEE
Sendai, Japan - September 13th to 18th 2020

A PREDICTIVE LOW-CYCLE FATIGUE MODEL FOR BUCKLING RESTRAINED BRACES

B. Saxey[1], Z. Vidmar[2], C.-H. Li[3], M. Reynolds[4], C.-M. Uang[5]

[1] *Technical Director, CoreBrace, USA, brandt.saxey@corebrace.com*
[2] *Senior Engineer, CoreBrace, USA, zac.vidmar@corebrace.com*
[3] *Graduate Student Researcher, University of California, San Diego, USA, chl228@eng.ucsd.edu*
[4] *Graduate Student Researcher, University of California, San Diego, USA, mpreynol@eng.ucsd.edu*
[5] *Professor, Department of Structural Engineering, University of California, San Diego, USA, cmu@ucsd.edu*

Abstract

Buckling-Restrained Brace Frame (BRBF) has been a popular seismic force-resisting system since it was first introduced to the AISC Seismic Provisions (or AISC 341) and ASCE 7 in 2005. The steel core of a buckling-restrained brace (BRB) yields in tension and develops a high-mode local buckling mode in compression under cyclic loading. Prequalification testing of BRBs in conformance with the AISC 341 requirements relies on a highly idealized symmetric loading protocol that is not typical of the expected response during an earthquake. Although testing has demonstrated that BRBs have excellent energy dissipation capacity, a low-cycle fatigue model is needed so designers may evaluate the remaining life of BRBs after a seismic event. To develop and validate such model, 18 large-capacity BRBs in groups of 3 different yielding strengths (nominally 1,110, 2,220, and 3,330 kN, respectively) were cyclically tested to fracture with the following loading conditions: (a) symmetric cycles with constant strain ranges (0.5%, 1.5%, 4% and 6%), (b) symmetric cycles with variable strain ranges, and (c) simulated earthquake responses. The damage model was first developed from 11 tests with the loading condition (a); the model was established by considering the low-cycle fatigue characteristics of both the elastic and plastic components of each BRB. This model was then validated with two specimens that were tested with the loading condition (b). To validate the model for earthquake-type random excitations, responses from three specimens that were tested with the loading condition (c) with simulated near-fault and far-field time history responses were used. In addition, three nominally identical specimens were tested with a strain range of 0.05 mm/mm but with a modified loading condition (a) to evaluate the effect of mean strain (0.01 mm/mm in either tension of compression). The proposed model allows for resiliency checks of existing or planned BRBFs.

Keywords: Buckling-Restrained Brace, BRB, BRBF, Fatigue

1. Introduction

Extensive research including component and system-level testing has demonstrated that buckling-restrained braced frame (BRBF) is a reliable seismic force-resisting system [1, 2]. As a result, BRBF has gained acceptance for new construction or seismic retrofit of buildings and other structures in high seismic regions in the world. BRBFs are expected to provide significant inelastic deformation capacity primarily through buckling-restrained braces (BRBs). Under seismic loading, the steel core of a BRB yields in tension and develops a high-mode local buckling mode in compression to ensure yielding of the steel in compression. Although results from numerous testing showed that a BRB can easily meet the siesmic demand from a significant seismic event, it is highly desirable that a low-cycle fatigue be established such that an engineer can make a decision after an earthquake if BRBs need to repalced. But research on this subject is limited. Based on the test results from five separate studies in Japan, Takeuchi et al. [3] developed a model to estimate the cumulative deformation capacity of BRBs. The imposed atrain amplitude of their fatigue tests was in a range from ±1.0% to ±2.5%. Reduced-scale BRB specimens were used; the length of the steel core ranged from 480 mm to 1,610 mm, and the nominal yielding strength ranged from 120 to 670 kN. Of a total of 20 specimens considered in the study, 15 specimens were fabricated with low-yield steel (specified ultimate strength ranging from 200 to 400 MPa and the elongation ranging from 40% to 50%. Since the majority of the BRB specimens were made from low-yield steel, which is not commonly used in the U.S., fatigue tests were conducted on eighteen full-scaled BRBs at the University of Calfornia, San Diego. The length of the steel core was about 5,400 mm, and the nominal yield strength ranged from 1,110 to 3,330 kN, significantly higher than those studied by Takeuchi et al. In addition, this program conducted a fatigue test with a strain amplitude of ±3.0%, which is beyond the scope of the previous reseach. Based on the test results in this study, a low-cycle fatigue life assessment method is developed and the effectiveness of the method is experimentally verified.

2. Test Program

Three sets of nominally identical BRB specimens for a total of eighteen BRB specimens were tested. The three sets (Series A, B, and C) had incrementally larger core cross-sectional areas (A_{sc}) with an expected yield strength (P_{ye}) of 1110, 2220, and 3330 kN, respectively. The steel cores and steel casing were manufactured with A36 and A500 Gr. B steel, respectively. Table 1 depicts the test matrix. The fatigue tests can be divided into two groups: “constant-amplitude” and “variable-amplitude” tests.

The constant-amplitude tests can be further categorized into two types: cyclic tests with “symmetric” and “shifted-symmetric” strain cycling (See Fig. 1a). There were 11 specimens tested with symmetric strain cycles to fracture. Within each set, three specimens were tested with a constant-amplitude of ±0.25%, ±0.75% and ±2.0% core strains, respectively Two additional specimens in the B series were tested with higher strains (±2.5% and ±3.0%). In addition, there were two specimens in the B series tested with “shifted-symmetric” strain cycles (See Fig. 1b). Specimen B7 was subjected to the constant-amplitude strain cycles with the compressive and tensile strain peaks at -1.5% and +3.5%, respectively; Specimen B8 was tested with the compressive and tensile strain peaks at -3.5% and +1.5%, respectively. These two shifted-symmetric strain cycling test specimens were subjected to a constant strain range of 5% for each strain excursion during the test, which is the same as the strain range imposed on the symmetric strain cycling test specimen B6. A comparison of these three specimens can be used to evaluate the mean strain effect on BRB fatigue behavior. In order to simulate the strain rate effect expected in an earthquake, cyclic testing was conducted in a dynamic manner such that the imposed strain rate reached about 0.75%/s for ±0.25% cycle tests and as high as 5.0%/s for the other constant-amplitude cycle tests.

In the variable-amplitude test group, two specimens were tested with the variable-amplitude symmetric cycles during the test. Specimen A5 was tested with a modified AISC loading protocol. The AISC loading protocol, prescribed in Section K3 of the AISC Seismic Provisions [4], was modified such that the repeated constant cycles at the end of the loading protocol were not performed-as the minimum culmutive inelastic deformation requirment was met with the ramped cycles. Instead, the ramped 5 discrete strain levels of the AISC protocol (±0.15%, ±0.5%, ±1.0%, ±1.5% and ±2.0%), which were performed for two cycles at each strain level, were repeated until the specimen failed. Specimen C5 was subjected to a two-phase constant-

amplitude test with symmetric cycles. It was first subjected to a total of 1,000 cycles of ±0.25% constant-amplitude strain before ±0.75% constant-amplitudes cycles were applied until fracture.

Another type of variable-amplitude test is the simulated earthquake loading test. In each of the three series in Table 1, the fourth specimen was subjected to simulated earthquake responses that were repeated until fracture. These specimens were designated with "EQ". Nonlinear time-history analyses were performed on an example 4-story BRBF (4F-BRBF) building in the AISC Seismic Design Manual [5] to generate the BRB core strain histories. The nonlinear structural analysis software PISA3D [6] was used for the analyses. The simulated core strain history was obtained from the predicted responses of the first-story BRBs in the example frame. Specimen A4 was subjected to a California earthquakes loading sequence, named EQ1. The simulated core strain history was obtained from a combination of two separate frame analyses with the following input motion: (a) a 1989 Loma Prieta earthquake record scaled to 120% of the maximum considered earthquake (MCE) level, and (b) a record form the 1999 Hector Mine earthquake scaled to the MCE level (See Fig. 1c). Specimen B4 was repeatedly tested with the loading sequence EQ2, which was composed of two simulated earthquake responses. The first half is generated from a near-fault record ('Sylmar-Converter Station') from the 1994 Northridge earthquake scaled to the MCE level, and the second half is identical to the first half but with the sign reversed (See Fig. 1d). Specimen C4 was repeatedly tested with the loading sequence EQ3, which was composed of three MCE level earthquake responses (See Fig. 1e): (a) a record ('Gilory Array #6') from the 1989 Loma Prieta earthquake, (b) a record ('Kekerengu Valley Road') from 2016 Amberley earthquake (New Zealand), and (c) a record ('La Union, Guerrero Array') from 1995 Michoacán earthquakes (Mexico). In all cases, the values of the spectral response acceleration parameters S_{DS} = 1.0 and S_{D1} = 0.6 were used to define the MCE design spectrum [7].

Table 1 – Test matrix

Series	Specimen Designation	BRB Properties			Constant-amplitude Tests	Variable-amplitude Tests
		A_{sc} (mm^2)	P_{ye} (kN)	L_b (mm)	Strain Amplitude (mm/mm)	Loading Protocol Description
A	A1	3,652	1,110	5,477	±0.25%	-
	A2				±0.75%	-
	A3				±2.00%	-
	A4				-	Simulated Earthquake (EQ1)[1]
	A5				-	Modified AISC Protocol
B	B1	7,232	2,200	5,461	±0.25%	-
	B2				±0.75%	-
	B3				±2.00%	-
	B4				-	Simulated Earthquake (EQ2)[2]
	B5				±3.00%	-
	B6				±2.50%	-
	B7				–1.50%/+3.50%	-
	B8				–3.50%/+1.50%	-
C	C1	11,135	3,300	5,424	±0.25%	-
	C2				±0.75%	-
	C3				±2.00%	-
	C4				-	Simulated Earthquake (EQ3)[3]
	C5				-	Two-phase Constant-Amplitude

1. 1989 Loma Prieta (120% MCE) and 1999 Hector Mines (100% MCE)
2. 1994 Northridge (100% MCE)
3. 1989 Loma Prieta, 2016 Amberley (NZ), and 1985 Michoacán (Mexico) (All three are scaled to100% MCE)

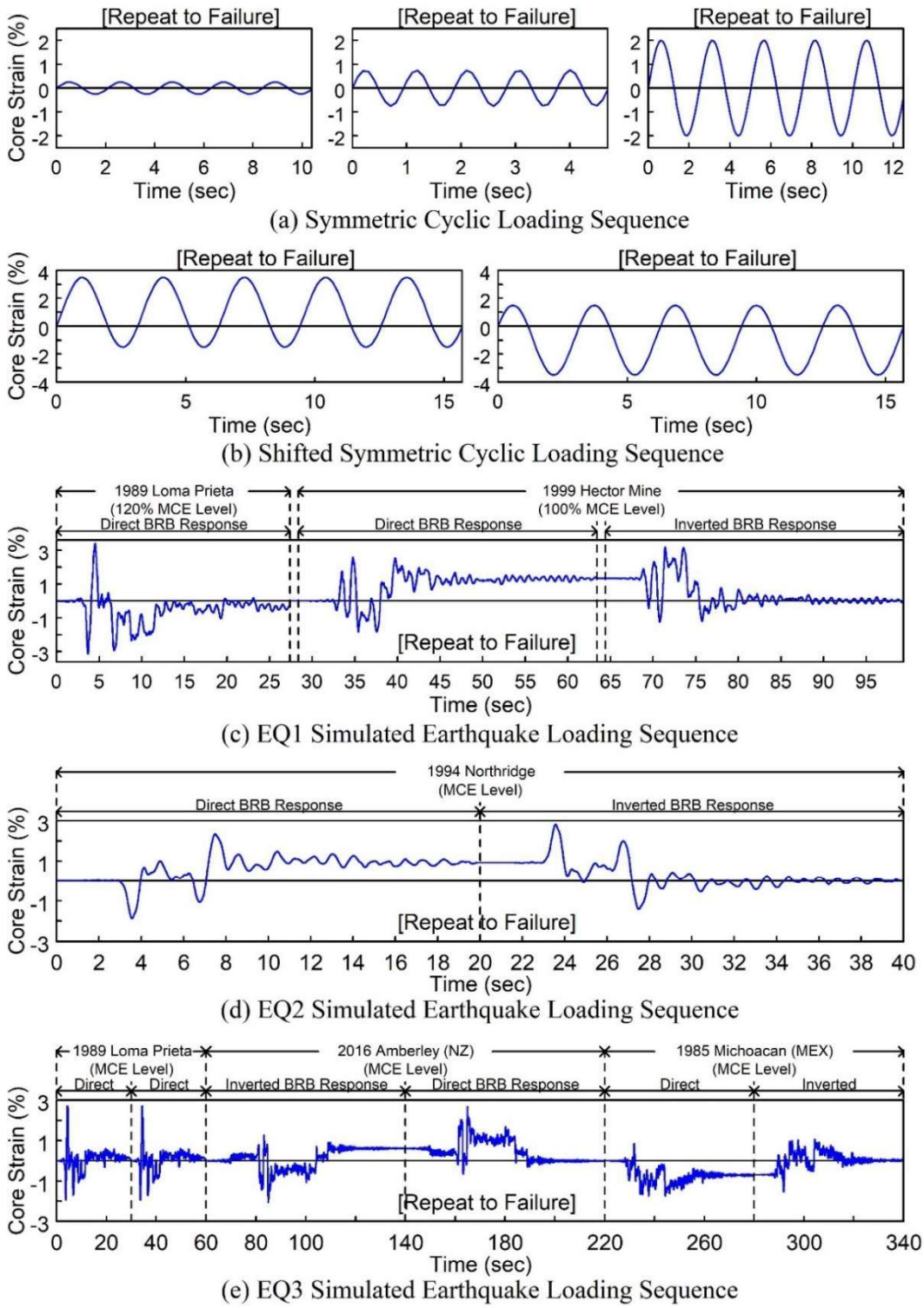

Fig. 1 – Loading sequences: (a) symmetric constant-amplitude cycles; (b) shifted-symmetric constant-amplitude cycles; (c) EQ1; (d) EQ2; and (e) EQ3

Table 2 – Constant-amplitude test results

Specimen Designation	Target Strain Range (%)	Target Strain Amplitude (%)	Number of Completed Cycles to Failure	Number of Rain-flow Cycles to Failure, N_f	Average Total Strain Range, $\overline{\Delta\varepsilon_t}$ (%)	Cumulative Inelastic Deformation, η
A1	0.5	±0.25	2,072	2,072.5	0.509	5,573
B1			2,346	2,346.5	0.530	6,780
C1			2,278	2,278.5	0.519	6,719
A2	1.5	±0.75	201	201.5	1.568	3,346
B2			174	174.5	1.570	2,867
C2			243	243.5	1.517	3,957
A3	4.0	±2.0	16	16.5	4.027	808
B3			22	22.5	4.153	1,126
C3			31	31.5	3.956	1,542
B6	5.0	±2.5	11	11.5	4.936	694
B7*		–1.50/+3.50	14	14.5	4.934	875
B8*		–3.50/+1.50	10	10.5	4.846	624
B5	6.0	±3.0	9	9.5	5.855	687

*Shifted symmetrical cyclic tests

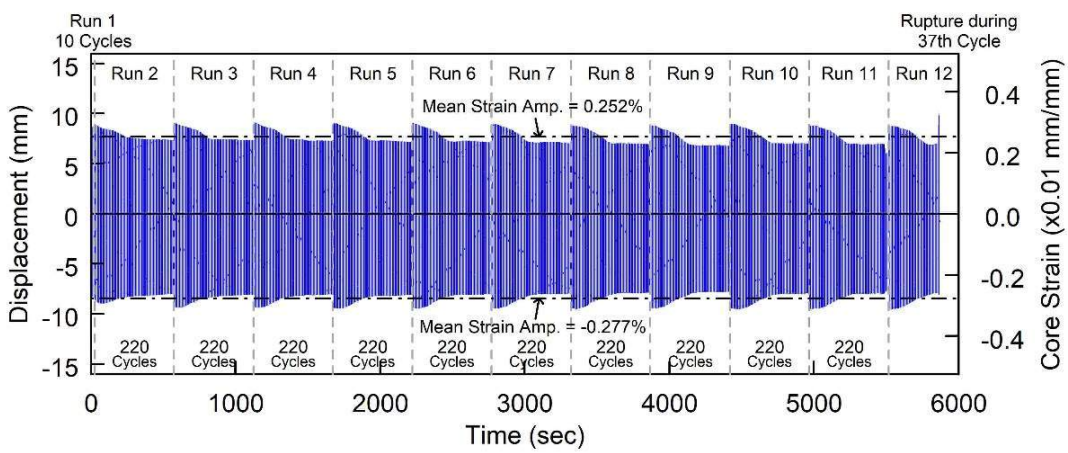

Fig. 2 – Sample BRB axial displacement history (Specimen 2220-0.25)

3. Test Results

Table 2 summarizes results of the constant-amplitude tests. It is found that the BRB fatigue lives under the ±0.25%, ±0.75% and ±2.0% strain amplitudes were on the order of 2,000, 200 and 20 cycles, respectively. Based on the limited test data, the BRB constant-amplitude fatigue life for the ±2.5% and ±3.0% strain amplitude would be 11 and 9 cycles, respectively.

Figure 2 shows the measured axial displacement time history and the associated average core strain time history of a sample specimen (Specimen B1). The average core strain, ε, is defined as Δ_b/L_y, where Δ_b and L_y are the measured brace displacement and the length of the steel core plate in the yielding zone, respectively. For high-capacity braces that required a large number of cycles at the lower strain amplitudes (±0.25% and

±0.75% in this experimental program), testing had to be conducted at intervals due to hydraulic limitations of the shake table test facility used. The figure shows that the entire fatigue test for this specimen was completed by 12 separate test runs. Except for the first trial test run and the last test run in which the rupture occurred, each of the other test runs had 220 cycles. Hydraulic limitations resulted in a minor deviation of imposed strain amplitudes during each test run; however, the mean strain amplitude in both tension and compression directions matched the target strain amplitude (See Figure 2).

Figure 3 shows sample hysteretic responses of the B Series specimens under the constant-amplitude tests. Table 2 also lists the normalized cumulative inelastic deformation (η_D) for the constant-amplitude test specimens. The normalized total inelastic axial deformation for the *i*-th cycle, μ_i, with a deformation level greater than the yield deformation is given by:

$$\mu_i = \frac{2|\Delta_i^+ - \Delta_i^-|}{\Delta_{by}} - 4 \tag{1}$$

where Δ_i^+ and Δ_i^- are the values of maximum and minimum deformations for the *i*-th cycle, respectively, and Δ_{by} is the BRB deformation corresponding to the yielding of the brace. The cumulative inelastic axial deformation, η, is then computed as the sum of the normalized inelastic axial deformation for each cycle:

$$\eta = \sum \mu_i \tag{2}$$

For uniaxial testing of BRBs, the AISC Seismic Provisions [4] require that the cumulative inelastic axial deformation (η) reach a value of at least 200. The value of η of the ±0.25% constant-strain specimens reached from 5,600 to 6,800. The ±0.75% strain specimens withstood a η value ranging from 2,900 to 4,000. The specimens with ±2.0% strains sustained values of η between 800 and 1,500. When the strain amplitude was increased to ±2.5% and ±3.0%, the BRB still developed a η of 694 and 687, respectively.

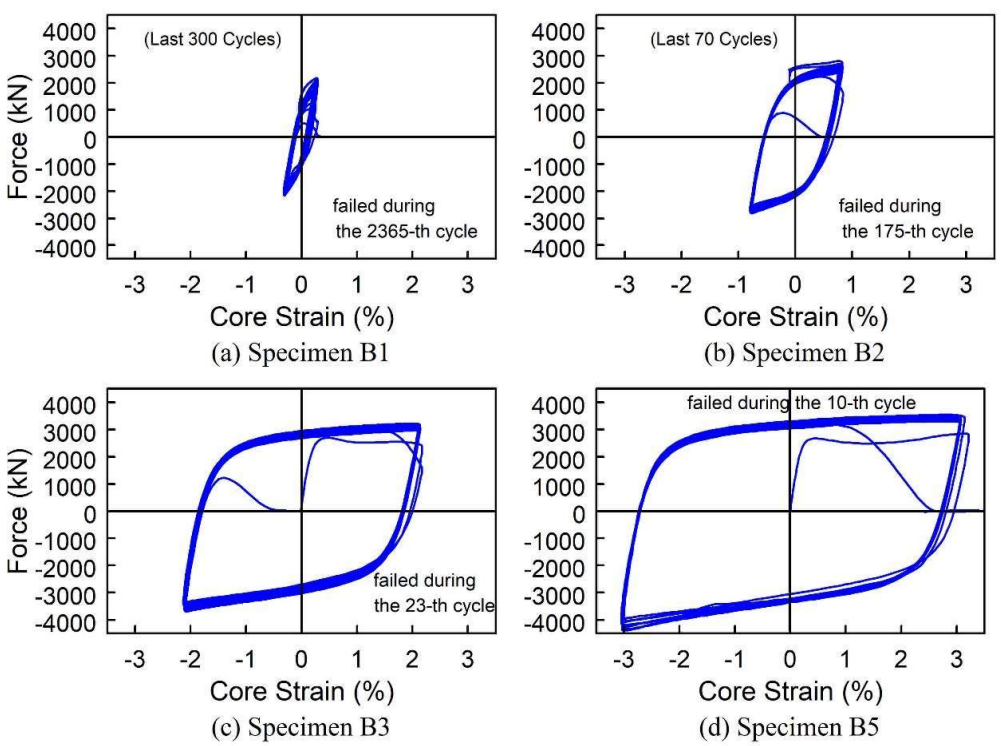

Fig. 3 – Hysteretic responses of B series specimens (symmetric constant-amplitude tests)

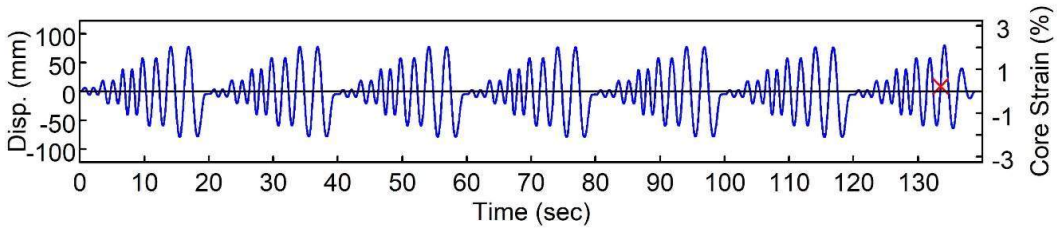

(a) Specimen A5 (Modified AISC Loading Sequence)

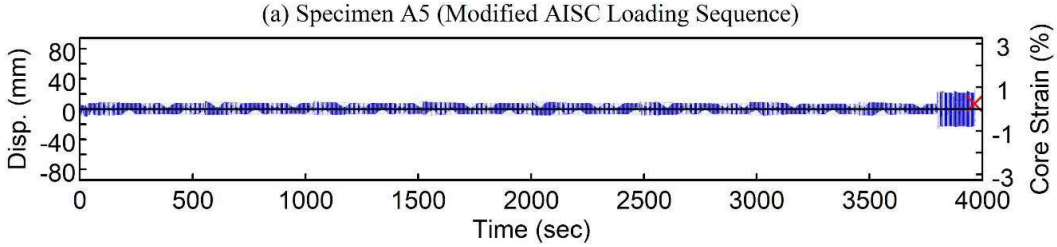

(b) Specimen C5 (Two-Phase Constant-Amplitude Loading Sequence)

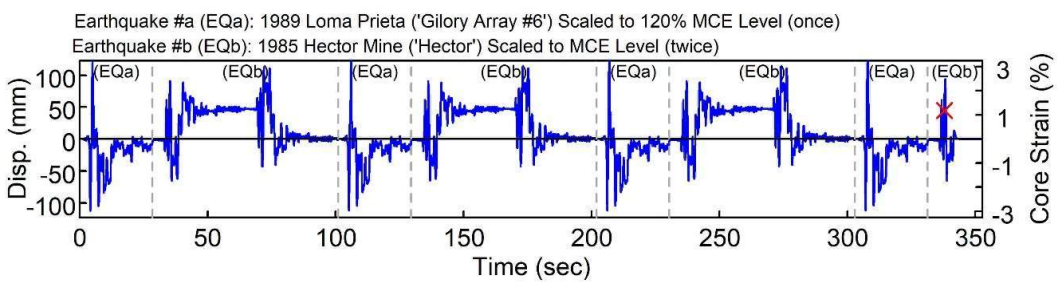

(c) Specimen A4 (Simulated California Earthquakes Loading Sequence)

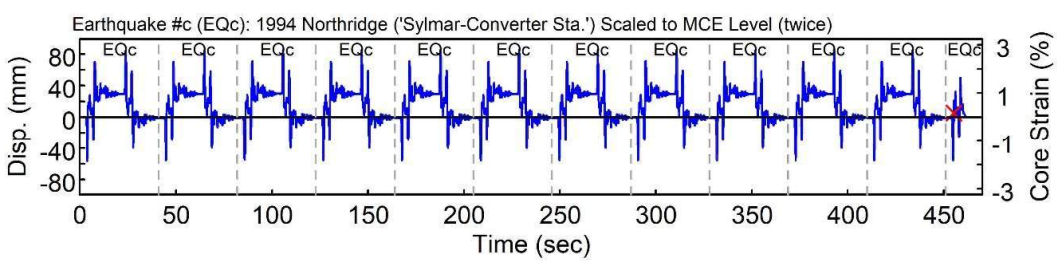

(d) Specimen B4 (Simulated Northridge Earthquake Loading Sequence)

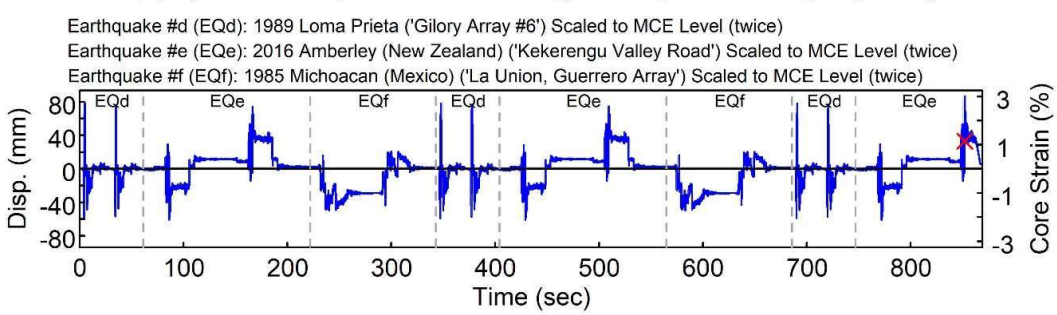

(e) Specimen C4 (Simulated Worldwide Earthquakes Loading Sequence)

Fig. 4 – Displacement time histories of variable-amplitude tests: (a) Specimen A5; (b) Specimen C5; (c) Specimen A4; (d) Specimen B4; and (e) Specimen C4

Figure 4 shows the core strain time histories of variable-amplitude tests. Specimen A5 completed 6 test runs of the modified AISC protocol and fractured during the first 2.0% cycle of the 7th test run (Fig. 4a); the η value reached 1,580 at rupture. Specimen C5 first completed 1,000 cycles of ±0.25% strain amplitude, followed by another 113 cycles of ±0.75% strain cycles before fracture (Fig. 4b). The specimen developed a η value of 5,033, of which the ±0.25% strain-amplitude cycles contributed 62.5% of η and the ±0.75% strain cycles contributed the remaining. Figures 4c to 4e show the core strain time histories of the three specimens tested with simulated earthquake responses. Specimens A4, B4, and C4 generated η values of 1,584, 1,592, and 998, respectively. It is noted that each of these three specimens survived the simulated MCE response more than 10 times.

4. Low-cycle Fatigue Life Assessment Method

The 11 symmetric, constant-amplitude cyclic test results were used to establish a low-cycle fatigue life assessment model. A procedure used to establish the fatigue model for the base metal [8] was adopted herein for the BRBs. For each half cycle of the hysteresis loops, the total strain range ($\Delta\varepsilon_t$), was separated into the elastic ($\Delta\varepsilon_e$) and plastic ($\Delta\varepsilon_p$) components. The total strain range was the strain excursion from the tension to compression strain peaks or that from compression to tension strain peaks. In addition, the average stress of the steel core was calculated by dividing the brace axial force by the core area A_{sc}. The elastic strain range component, $\Delta\varepsilon_e$, was obtained by dividing the absolute stress amplitude difference between the tension and compression strain peaks by the Young's modulus, E. Finally, the plastic component, $\Delta\varepsilon_p$, was computed as $\Delta\varepsilon_t - \Delta\varepsilon_e$.

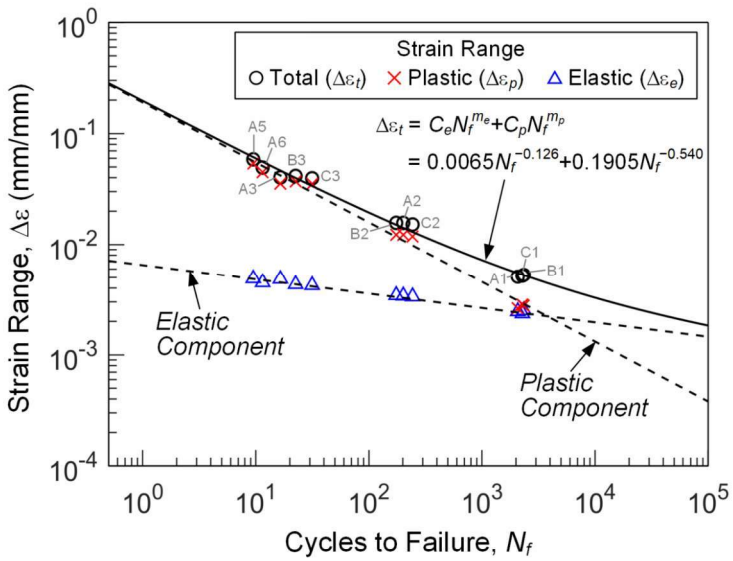

Fig. 5 – Fatigue curves based on symmetric, constant-amplitude cyclic test results

Considering the results of all eleven symmetric, constant-amplitude tests, Figure 5 shows that the relationship between the elastic strain range, $\Delta\varepsilon_e$, and the number of cycles to failure (N_f) could be approximated by a linear relationship in a log-log plot. The same linear trend was also observed between the plastic strain range, $\Delta\varepsilon_p$, and N_f. Regression analyses were conducted to establish the relationships between both the elastic and plastic strain ranges and the number of cycles to failure, which yield the following results:

$$\Delta\varepsilon_e = C_e {N_f}^{m_e} = 0.0065 {N_f}^{-0.126} \quad (3)$$

$$\Delta\varepsilon_p = C_p {N_f}^{m_p} = 0.1905 {N_f}^{-0.540} \tag{4}$$

where C_e and m_e are the constants for the $\Delta\varepsilon_e$ versus N_f relationship, and constants C_p and m_p are for the $\Delta\varepsilon_p$ versus N_f relationship. Then the fatigue model relating the total strain range to the number of cycles to failure is:

$$\Delta\varepsilon_t = \Delta\varepsilon_e + \Delta\varepsilon_p = C_e {N_f}^{m_e} + C_p {N_f}^{m_p} = 0.0065 {N_f}^{-0.126} + 0.1905 {N_f}^{-0.540} \tag{5}$$

where $\Delta\varepsilon_t$, $\Delta\varepsilon_e$, and $\Delta\varepsilon_p$ are in mm/mm, not % of mm/mm. Since the imposed strain amplitude varied mildly during testing, the rain-flow counting method [9] was employed to do the cycle counting for these constant-amplitude tests. It should be noted that the proposed fatigue mode herein was developed from the number of cycles to failure and the averaged strain ranges determined from the rain-flow method.

The variable-amplitude test results were used to verify the effectiveness of the proposed low-cycle fatigue method. The rain-flow counting method was employed for the variable-amplitude tests to extract the number of cycles and their respective strain ranges. After applying the rain-flow counting, the entire loading history could be analyzed as a series of full-cycles and a series of half-cycles. Each full-cycle or half-cycle has its own corresponding total strain range, $\Delta\varepsilon_t$. The rain-flow counting results were then used in the calculation of the Miner's damage index, *D* [10]. The proposed calculation method is:

$$D = \sum_{i=1}^{n} \frac{n_i}{N_{fi}} = \sum_{j=1}^{N_{full}} \frac{1}{N_{fj}} + \frac{1}{2}\left[\sum_{k=1}^{N_{half}} \frac{1}{N_{fk}}\right] \tag{6}$$

with

$$\begin{aligned} \Delta\varepsilon_{tj} &= 0.0065 {N_{fj}}^{-0.126} + 0.1905 {N_{fj}}^{-0.540} \\ \Delta\varepsilon_{tk} &= 0.0065 {N_{fk}}^{-0.126} + 0.1905 {N_{fk}}^{-0.540} \end{aligned} \tag{7}$$

where N_{full} and N_{half} are the numbers of full-cycles and half-cycles, respectively. $\Delta\varepsilon_{tj}$ and $\Delta\varepsilon_{tk}$ represent the strain ranges corresponding to the *j*-th full-cycle and the *k*-th half-cycle, respectively. Given $\Delta\varepsilon_{tj}$ and $\Delta\varepsilon_{tk}$, Equation (7), which the same as Eq. (5), can be solved for the predicted number of cycles to failure, N_{fj} and N_{fk}. The excursion of a full-cycle of strain range $\Delta\varepsilon_{tj}$, was assumed to generate a damage or *D* value of $1/N_{fj}$, and the excursion of a half-cycle of strain range $\Delta\varepsilon_{tk}$ would consume a fatigue life of $1/(2N_{fk})$. A value of *D* reaching 1.0 would predict the BRB fractures.

5. Verification of Assessment Method

Based on the proposed calculation procedure, Table 3 lists the *D* values for the symmetric, constant-amplitude cyclic test specimens. A *D*-index smaller than 1 represents that the BRB specimen ruptured earlier than the prediction, i.e., a non-conservative prediction. On the other hand, a *D*-index larger than 1 means that the BRB ruptured later than the prediction, i.e., a conservative prediction. Table 3 shows the *D*-index ranges from 0.76 to 1.41, with an overall mean value of 1.04 and a coefficient of variation (COV) of 22.5%. The proposed method tends to overestimate the fatigue life for the ±0.25% strain tests and underestimate those of the ±0.75% strain tests. The COV of *D*-index for these two groups of specimens were about 12%. The proposed model predicts the ±2.0% strain tests the best with a mean *D* value of 1.08 but the COV is 29.5%, suggesting that the variation of the fatigue performance would increase with the strain amplitude.

Table 3 – *D*-indices for symmetric, constant-amplitude cyclic test specimens

Target Strain Amplitude	Specimen Designation	*D*-index	Average *D*-index	Coefficient of Variation (COV)
±0.25%	A1	0.78	0.90	11.9%
	B1	1.00		
	C1	0.92		
±0.75%	A2	1.26	1.25	12.7%
	B2	1.09		
	C2	1.41		
±2.00%	A3	0.76	1.08	29.5%
	B3	1.09		
	C3	1.39		
±2.50%	B6	0.79	–	–
±3.00%	B5	0.93	–	–
			Avg. = 1.04 COV = 22.5%	

Table 4 – *D*-indices for variable-amplitude test specimens

Loading Type	Loading Sequence	Specimen Designation	*D*-index	Average *D*-index	Coefficient of Variation (COV)
Symmetric Cycles with Variable Amplitude	Repeated Modified AISC Protocol	A5	1.13	1.12	1.26%
	Two-phase Constant Amplitude	C5	1.11		
Simulated Earthquake Response	EQ1	A4	1.29	1.03	25.1%
	EQ2	B4	1.05		
	EQ3	C4	0.77		
			Avg. = 1.07 COV = 17.9%		

Table 4 shows that the *D*-indices for the variable amplitude tests range from 0.77 to 1.29. This is within the variation range observed from the constant-amplitude tests. Also, note that the mean value and COV of the *D*-indices are similar to those from the constant-amplitude tests. For the two symmetric loading tests with variable-amplitudes, Specimens A5 and C5, the *D*-indices are very close to 1.1 with a very small COV, indicating that the proposed method slightly overestimate the fatigue life for this type of loading history. For the earthquake loading tests, the prediction method still works reasonably well. The *D*-indices for Specimens A4, B4, and C4 are 1.29, 1.05, and 0.77, respectively, with a mean value of 1.08, although the prediction model overestimates the fatigue life of Specimen C4. This level of accuracy appears sufficient to provide practicing engineers with the information necessary to recommend reuse or replacement of a BRB after an earthquake if the displacement history of the BRB is measured.

Figure 6 shows the test results comparison of three Series B specimens subjected to 5% strain range cycles. Specimen B6, subjected to the symmetric, constant-amplitude ±2.5% strain cycles, withstood 11

completed cycles and ruptured just before the tensile strain peak in the 12th cycle was reached. Specimen B7 was tested with the shifted symmetric cycles with amplitude ranging from –1.5% to +3.5%, i.e., the loading history has a mean strain of +1.0% (in tension). The specimen survived 14 completed cycles. On the other hand, Specimen B8 was loaded in a manner similar to that of Specimen B7, the difference being that the amplitude ranged from –3.5% to +1.5% with a –1.0% mean strain (in compression). The specimen resisted only 10 cycles before fracture. Based on this limited database, it appears that the a mean tensile strain would increase the BRB fatigue life, but a mean compression strain mildly decreases the fatigue life. That is, compression strains are more detrimental to BRB fatigue life than tension strains. This can be explained, qualitatively, that a higher compression strain in the BRB results in a larger higher-mode buckling amplitude of the core plate, which introduces a significant local strain in the core plate. Also, the compressive strains tend to oblate microvoids which could excacerbate the ductile fracture process. Note that the proposed fatigue life assessment model does not take the mean strain effects into account because the assessment is made only by the strain ranges that a BRB experienced regardless of the relative strain amplitudes in the tensile and compressive directions. Thus, it is expected that the proposed assessment method will overestimate the BRB fatigue life for the core strain histories when the loading history has a mean compressive strain. Table 5 lists the *D*-indices for the three specimens with 5% strain range cycles. *D*-values of Specimens B8, B6, and B7 are 0.71, 0.79 and 1.01, respectively. The specimen B8 could represent a case with a relatively high compression mean strain in the earthquake engineering application. The proposed prediction method overestimates its fatigue life with a *D*-index of 0.71. Despite this, the extent of the overestimate appears acceptable for the engineering use.

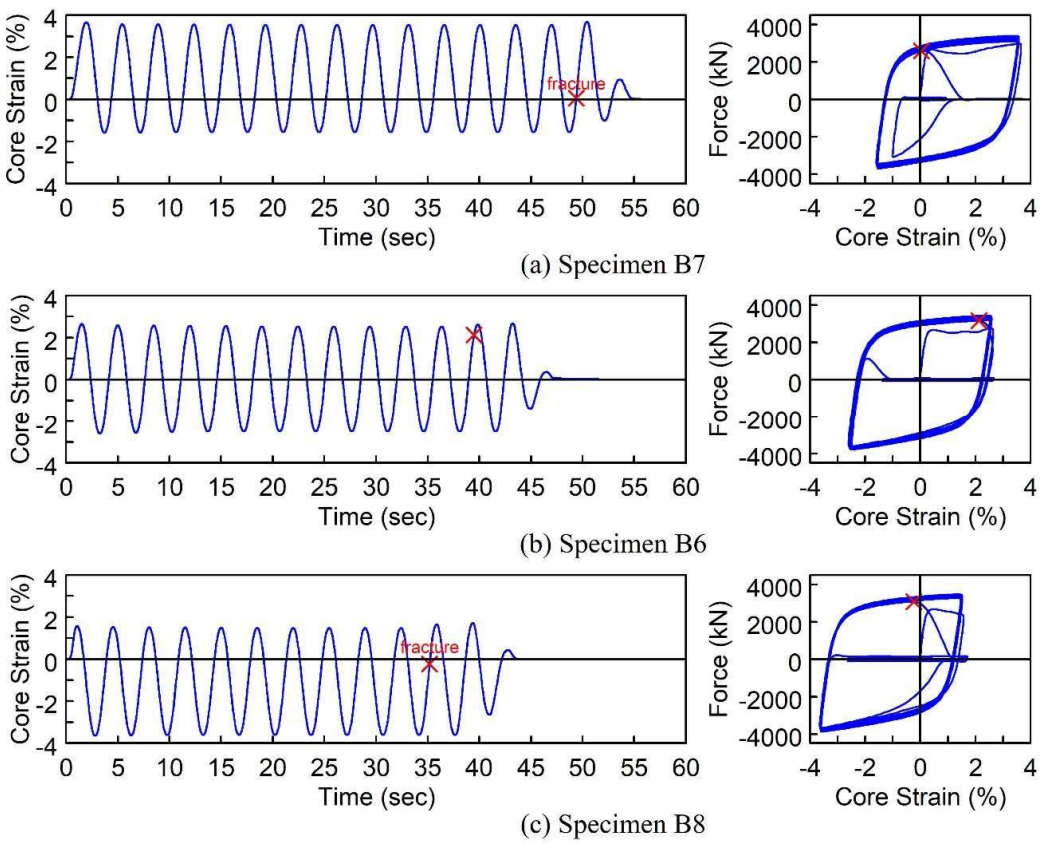

Fig. 6 – Comparison of test specimens subjected to 5% strain range cycles:
(a) Specimen B7; (b) Specimen B6; and (c) Specimen B8

Table 5 – *D*-indices for constant-amplitude test specimens with 5%-strain range cycles

Loading Type	Specimen Designation	Target Strain Range (%)	Target Strain Amplitude (%)	*D*-index
Symmetric Cycles	B6	5.0	±2.5	0.79
Shifted-Symmetric Cycles	B7		–1.50/+3.50	1.01
	B8		–3.50/+1.50	0.71

6. Conclusions

Test results showed that BRB specimens had a cumulative-inelastic ductility much larger than that specified in the code. Symmetric constant amplitude test results were used to calibrate a low-cycle fatigue model. Variable-amplitude tests results have verified that the proposed fatigue model together with the Miner's damage index could assess the remaining fatigue life of BRBs under earthquake-generated loading with reasonable accuracy. Test results also demonstrate that tests conducted with a mean compressive strain were more detrimental to BRB fatigue life than when conducted under a mean tensile strain. To further improve the accuracy of the proposed model, future research should consider this effect.

7. References

[1] Uang CM, Nakashima M, Tsai KC (2004): Research and application of buckling-restrained braced frames. *Journal of Steel Structures*, Korean Society of Steel Construction, **4** (4), 301-313.

[2] Takeuchi T, Wada A (2017): *Buckling-restrained Braces and Applications*, The Japan Society of Seismic Isolation, Tokyo, Japan.

[3] Takeuchi T, Ida M, Yamada S, Suzuki K (2008): Estimation of Cumulative Deformation Capacity of Buckling Restrained Braces. *Journal of Structural Engineering (ASCE)*, **134**(5), 822-831

[4] AISC (2016): *Seismic Provisions for Structural Steel Buildings. ANSI/AISC 341-16*. American Institute of Steel Construction, Chicago, IL.

[5] AISC (2018): *Seismic Design Manual,* 3rd Edition. American Institute of Steel Construction, Chicago, IL.

[6] Lin BZ, Chuang MC, Tsai KC (2009): Object-oriented Development and Application of a Nonlinear Structural Analysis Framework. *Advances in Engineering Software*, **40**(1), 66-82.

[7] ASCE (2016): *Minimum Design Loads for Buildings and Other Structures, ASCE/SEI 7-16*. American Society of Civil Engineers, Reston, VA.

[8] Raske DT, Morrow J (1969): Mechanics of Materials in Low Cycle Fatigue Testing. *Manual on Low Cycle Fatigue Testing*, *ASTM STP 465*, 1-25.

[9] Matsuishi M, Endo T (1968): Fatigue of Metals Subjected to Varying Stress, *Japan Society of Mechanical Engineers*, Jukvoka, Japan.

[10] Miner MA (1945): Cumulative damage in fatigue. *Journal of Applied Mechanics*. **12**, 159-164.